I&EC research
Industrial & Engineering Chemistry Research
Article
pubs.acs.org/IECR

Characterization of Aluminum-Neutralized Sulfonated Styrenic Pentablock Copolymer Films

Geoffrey M. Geise,[†] Carl L. Willis,[‡] Cara M. Doherty,[§] Anita J. Hill,[§] Timothy J. Bastow,[§] Jamie Ford,[∥] Karen I. Winey,[∥] Benny D. Freeman,[†] and Donald R. Paul*[,†]

[†]Department of Chemical Engineering, The University of Texas at Austin, 1 University Station C0400, Austin, Texas 78712, United States

[‡]Kraton Performance Polymers, Inc., 16400 Park Row, Houston, Texas 77084, United States

[§]CSIRO Materials Science and Engineering & CSIRO Process Science and Engineering, Private Bag 33, South Clayton MDC, Clayton, Victoria 3169, Australia

[∥]Department of Materials Science and Engineering, University of Pennsylvania, 3231 Walnut Street, Philadelphia, Pennsylvania 19104, United States

ABSTRACT: Suspension-phase neutralization of an acid-form sulfonated styrenic pentablock copolymer was used to prepare aluminum cross-linked polymer films. Aluminum neutralization was confirmed by ^{27}Al solid state NMR, and the aluminum-neutralized polymer resisted ion exchange to the sodium counterion form when the polymer was soaked in 1 mol/L sodium chloride for 30 days. The effects of aluminum neutralization on polymer morphology, mechanical properties, water and salt transport properties, and free volume were explored. The primary spacing of the morphology, as measured by small-angle X-ray scattering (SAXS), decreased upon neutralization of the sulfonated polymer. The hydrated aluminum-neutralized polymer was mechanically stronger than the non-neutralized polymer, but the dry aluminum-neutralized polymer was more brittle than the non-neutralized polymer. Neutralization of the polymer's sulfonic acid functionality resulted in a 5.5-fold decrease in water uptake. This water uptake decrease upon aluminum neutralization resulted in a decrease, relative to the non-neutralized polymer, in water and sodium chloride permeability and water vapor transport rate. These decreases in transport rates and water uptake were consistent with one another, based on an analysis of changes in free volume of the material upon aluminum neutralization. Sodium chloride permeability of the aluminum-neutralized polymer was less dependent on salt concentration than that of the non-neutralized polymer, which is consistent with neutralization of the polymer's charged sulfonate groups. Aluminum neutralization increased the polymer's water/sodium chloride permeability selectivity because of a 1.8-fold increase in the material's diffusion selectivity. Free volume element size, characterized by *ortho*-positronium lifetime, decreased upon aluminum neutralization in both dry and hydrated film samples.

■ INTRODUCTION

Sulfonated polymers have been considered for a variety of applications such as ion exchange resins, fuel cell membranes, dehydration membranes, water-treatment membranes, and cation exchange membranes in electrodialysis and reverse electrodialysis systems.[1−12] Material properties must be tuned to achieve optimal performance for each application. The strongly acidic sulfonate groups of sulfonated polymers provide an opportunity for tailoring material properties by a variety of chemistries including metal ion neutralization, which can cause substantial variations in ion and water transport properties.[13−17]

Metal ion neutralization of an acid-form sulfonated polymer, or any cation exchange material, involves an ion exchange process, which is typically diffusion-limited, that replaces the protons on the sulfonic acid moieties in the sulfonated polymer (i.e., ionomer) with metal cations.[2] Such neutralization generally affects material properties for a variety of reasons.[5,16,18−22] A wide range of both mono- and multivalent ions can be used for neutralization, providing many opportunities to modify properties of such polymers.

When multivalent ions are used to neutralize an ionomer, ionic cross-linking can occur if the ions bond to charged functional groups attached to polymer chains.[23−25] An example of this cross-linking can be observed by contacting sodium alginate, a sodium-neutralized carboxylated polymer, with an aqueous solution of calcium chloride; calcium preferentially binds to the polymer's carboxylate groups and the cross-linked alginate gels rapidly.[26] Additionally, multivalent cation neutralization has been applied to a variety of polymers for gas separation,[25,27] pervaporation,[24,28] and facilitated transport[29−31] membrane applications.

The strength and stability of the bond between the neutralizing cation and the polymer's fixed charge group is important. Bonds between neutralizing cations and fixed charge groups on the polymer will be more stable if the bonds have covalent character. Furthermore, the dielectric constant of the swollen polymer is expected to be lower than that of pure water;[32,33] the tendency of a salt to dissociate decreases as the

Special Issue: Baker Festschrift

Received: November 7, 2011
Revised: January 31, 2012
Accepted: April 5, 2012
Published: April 5, 2012

dielectric constant decreases,[34] so the polymer environment can also act to stabilize the cross-linked bonds.[32] Bonds that are more ionic in nature are more likely to dissociate upon exposure to water or salt solutions than bonds that are more covalent in nature; in the case of multivalent cation neutralization, dissociation could disrupt polymer cross-links.

In this study, we report results from an experimental program to explore the influence of aluminum neutralization on the mechanical, morphological, and transport properties of a sulfonated pentablock copolymer. Aluminum was selected as the neutralizing cation because the aluminum-sulfonate group bond is stronger than that of some other sulfonate bonds to metal ions, such as potassium and calcium, that typically dissociate upon exposure to water.[35] The stability of the sulfonate group-aluminum bond can be understood by comparing the electronegativity values of the various atoms involved. The oxygen atoms in the sulfonate groups are highly electronegative, and the covalent nature, i.e. stability, of the sulfonate group-metal bond increases as the electronegativity of the metal increases.[36] The electronegativity of aluminum is 1.61.[37] Alkali and alkaline earth metals tend to be less electronegative than aluminum; electronegativity values for sodium, potassium, calcium, and magnesium are 0.93, 0.82, 1.00, and 1.31, respectively.[37] Bonds between sulfonate groups and alkali or alkaline earth metals will be more ionic than bonds between aluminum and sulfonate groups.[35,36] Therefore, polymer cross-links formed by aluminum neutralization are expected to be more stable in aqueous environments than cross-links formed by calcium or magnesium neutralization.

This study considers a symmetric sulfonated styrenic pentablock copolymer;[38−45] materials of this general structure are available commercially from Kraton Performance Polymers, Inc. (Houston, TX). The copolymer, whose structure is shown in Figure 1, has a hydrophilic middle block, composed of a styrene/styrene sulfonic acid random copolymer, surrounded by hydrophobic hydrogenated isoprene and *tert*-butylstyrene blocks. We report the effects of aluminum neutralization on morphology, water sorption, mechanical properties, water and ion transport properties, and free volume. The aluminum-neutralized polymer's properties are compared to those of the non-neutralized sulfonated polymer precursor, which is initially in the acid-form.

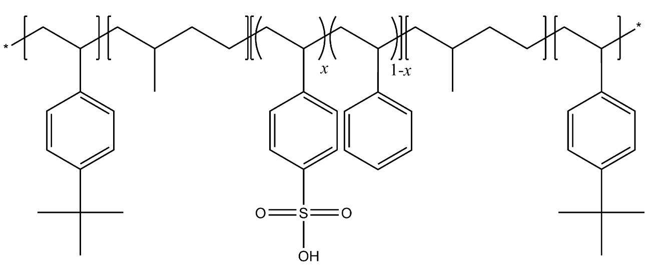

Figure 1. The acid-form symmetric sulfonated styrenic pentablock copolymer considered in this study shown with a degree of sulfonation *x*. Aluminum neutralization replaces some of the hydrogen atoms on the sulfonate groups with aluminum.

EXPERIMENTAL SECTION

Materials. The sulfonated styrenic pentablock copolymer (Figure 1) was prepared using anionic polymerization followed by catalytic hydrogenation of the residual isoprene C=C bonds.[38,40,41] The weight fractions of the unsulfonated symmetric copolymer poly(*tert*-butylstyrene), poly(hydrogenated isoprene), and poly(styrene) blocks were 0.33, 0.27, and 0.40, respectively,[43,44] and the total number average molecular weight of the polymer was approximately 78 kg/mol. The polymer was sulfonated to an ion exchange capacity of 2.0 milliequivalents (meq) per gram of dry polymer ($x = 0.52$ in Figure 1).[40,44] The material was prepared in the acid-form. Following synthesis and sulfonation, the polymer formed micelles at 10 wt % polymer in a 72:28 (by mass) heptane/cyclohexane solution.[42,46]

Aluminum neutralization was performed by adding triethylaluminum (Et_3Al) to a micellar suspension of 7:46:47 (by mass) polymer/heptane/cyclohexane under an inert atmosphere.[47] One mole of Et_3Al was added per equivalent of sulfonic acid. The neutralization reaction was exothermic, and a 20 °C rise in temperature was observed when 140 g of the polymer/solvent mixture was reacted. Presumably, each aluminum atom can bond to only one sulfonate group on any given polymer chain,[35] so this neutralization likely leads to cross-links involving, at most, three polymer chains per aluminum atom, as shown in Figure 2.[48,49]

Suspension-phase neutralization was preferred over neutralization of cast polymer films because restricted polymer chain motion in the solid state film can result in incomplete multivalent ion neutralization.[50] The micellar suspension did not appear to be affected by the neutralization reaction because no apparent increase in viscosity or color change was observed; consequently, neutralization of the sulfonate groups was believed to occur as Et_3Al diffused into the sulfonated core of the polymer micelles.[46] Since the suspension viscosity did not increase noticeably as a result of neutralization with aluminum, the polymer casting process was the same for both the aluminum-neutralized and the non-neutralized polymer.

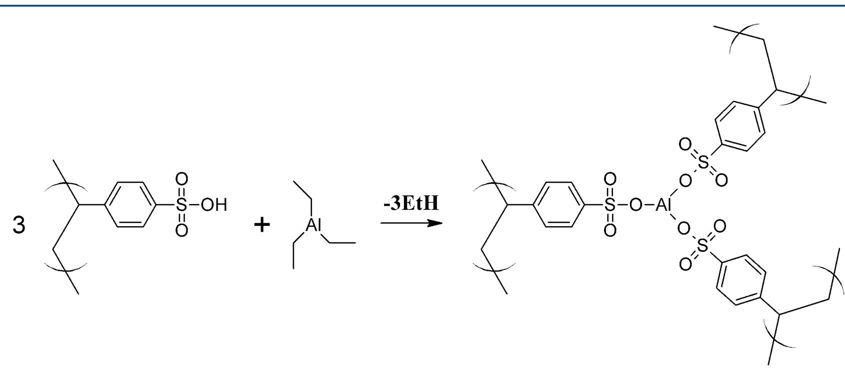

Figure 2. Theoretical completion of the aluminum neutralization and cross-linking of the sulfonated styrenic pentablock copolymer.

Transparent polymer films of uniform thickness were cast from the micellar suspension as described previously.[39] The polymer suspension was spread onto a silane-treated glass plate using a casting knife, and solvent was allowed to evaporate at ambient temperature in a nitrogen environment containing approximately 50% relative humidity.[39,44] Both the aluminum-neutralized and non-neutralized polymer films were cast to a dry film thickness of approximately 25 μm.

Solid State NMR. ^{27}Al magic angle spinning (MAS) NMR spectra were taken on a Bruker Avance 400 (Bruker, Alexandria, New South Wales, Australia) spectrometer in a nominal field of 9.395 T, at a frequency around 104.26 MHz, in a probe with a 4 mm rotor. The spectra were obtained using single pulse spectroscopy, with a MAS rotation frequency of 12.2 kHz. At this rotation frequency the innermost spinning side bands were well separated from any spectral features. The pulse repetition time for file acquisition was 0.2 s and 20,000 scans were accumulated. The reference zero ^{27}Al shift was that of the $Al(H_2O)^{3+}$ ion, set using a dilute aqueous solution of $AlCl_3$. The copolymer samples were equilibrated in air at ambient conditions prior to obtaining the spectra.

Small Angle X-ray Scattering. Small angle X-ray scattering (SAXS) experiments were performed using a multiangle X-ray scattering apparatus. Cu X-rays were generated using a Nonius FR 591 (Nonius/Bruker, Delft, The Netherlands) rotating-anode generator operated at 40 kV and 85 mA. The beam was obtained using pinhole optics in an integral vacuum system. The scattering data were collected using a Bruker Hi-Star two-dimensional detector with a sample-to-detector distance of 150 cm. The isotropic 2-D data were integrated into 1-D plots using the Datasqueeze software package.[51] The film's primary feature spacing, d, was obtained from the scattering vector at maximum scattering intensity, Q^*

$$d = \frac{2\pi}{Q^*} \tag{1}$$

Polymer films were rinsed and equilibrated in deionized (DI) water[44] prior to the SAXS measurement. Water swollen films were loaded into water-filled glass capillaries, and SAXS spectra were taken through the plane of the film. Dry samples were prepared by placing the water swollen film in a 100 °C oven for 8 h under vacuum; after the drying process, the films were mounted onto an aluminum sample plate, and SAXS spectra were taken through the plane of the film.

Aluminum Leaching Experiment. The resistance of the aluminum-sulfonate group bonds to dissociation and ion exchange was probed by leaching experiments. DI water swollen aluminum-neutralized polymer samples were immersed in a known volume of 1.0 mol/L NaCl solution for a period of 2 days to simulate a highly saline feed that might be encountered in an application. This salt concentration was chosen so that the overwhelming concentration of sodium ions, present in the solution, would ion exchange with the aluminum if the sulfonate group-aluminum bonds dissociated. Following this initial soaking period, the excess solution was wiped from the polymer samples, and the films were immediately placed in a new solution of 1.0 mol/L NaCl for a period of 30 days.

If the sulfonate group-aluminum bonds dissociate and ion exchange to the sodium counterion form occurs during the leaching experiment, aluminum will diffuse out of the polymer into the soaking solution. The concentration of aluminum in the NaCl soaking solutions was measured using flame atomic absorption (flame AA) spectrophotometry (Varian AA240, Clayton South, Victoria, Australia). Flame AA samples and standards were prepared in 2% (v/v) nitric acid, and the NaCl concentration in the calibration standards was chosen to match the concentration of NaCl in the test samples.

Water Uptake. Polymer samples were rinsed and equilibrated in DI water,[44] and the wet mass, m_{wet}, of each sample was recorded after quickly wiping water from the film surfaces. Then, films were placed in covered Petri dishes and dried under vacuum at ambient temperature until the polymer mass stabilized (at least 24 h). Next, the mass, m_{dry}, of the dried films, typically 25−30 mg, was measured. The material's water uptake, WU, was calculated as follows

$$\text{Water Uptake} = \text{WU} = \frac{m_{wet} - m_{dry}}{m_{dry}} \tag{2}$$

The mass concentration of water in the hydrated polymer sample, C_{w0}^{m}, was calculated from measured water uptake data, mass fractions, w_i, and corresponding densities, ρ_i, of each component in the swollen copolymer film as described in the literature[44]

$$C_{w0}^{m} = (\text{WU})\rho_m = \frac{m_{wet} - m_{dry}}{m_{dry}\left(\frac{w_{tBS}}{\rho_{tBS}} + \frac{w_{HI}}{\rho_{HI}} + \frac{w_S}{\rho_S} + \frac{w_{SS}}{\rho_{SS}} + \frac{\text{WU}}{\rho_w}\right)} \tag{3}$$

where ρ_m is the density of the swollen polymer film calculated by assuming volume additivity. The densities used in eq 3 are as follows: poly(*tert*-butylstyrene), ρ_{tBS} = 0.947 g cm^{-3},[52] poly(hydrogenated isoprene), ρ_{HI} = 0.85 g cm^{-3},[53] poly(styrene), ρ_S = 1.048 g cm^{-3},[52] poly(styrene sulfonic acid), ρ_{SS} = 1.47 g cm^{-3},[54] and water, ρ_W = 1.00 g cm^{-3}.[37] This approach to estimating the polymer's density was validated by measuring the acid-form polymer's dry density based on Archimedes' principle.[55] An analytical balance (Mettler Toledo XS205, Columbus, OH) was used in conjunction with a Mettler Toledo density determination kit. Since the sulfonated pentablock copolymers contain both hydrophilic and hydrophobic segments, a perfluorinated alkane, 3 M Fluorinert FC-77, was used as the auxiliary liquid, since it sorbs into the polymer to a negligible extent during the time scale of the experiments.[55] The measured density of the dry acid-form polymer was 1.10 ± 0.01 g/cm^3; this value compares reasonably well to the value estimated from eq 3, which was 1.06 g/cm^3. The measured dry density of the aluminum-neutralized polymer was 1.20 ± 0.03 g/cm^3. The increase in density upon aluminum neutralization is likely localized to the styrenic blocks where most of the aluminum atoms should be located.

The mass concentration of water in the hydrated polymer sample can be used to determine the water sorption coefficient, K_w, as shown below[13,56]

$$K_w \equiv \frac{C_{w0}^{m}}{C_{w0}^{s}} \tag{4}$$

where C_{w0}^{S} is the concentration of water in the solution used to equilibrate the polymer sample during the water uptake experiment. The value of C_{w0}^{S} was taken to be 1.00 g cm^{-3} for pure water at 25 °C.[37] The water sorption coefficient is useful for describing water permeability, P_w, in terms of solubility and diffusivity as expressed by the solution-diffusion model[57,58]

$$P_w = K_w D_w \tag{5}$$

where D_w is the apparent, concentration averaged water diffusion coefficient.

Tensile Property Characterization. Tensile mechanical properties were measured according to ASTM D 412.[59] Dumbell samples were cut from cast polymer films using a die and press. Both wet and dry samples were evaluated. Here, "dry" refers to films cast from hydrocarbon solvents as described earlier and then exposed to a laboratory atmosphere (nominally 25 °C and 50% RH) prior to and during testing. "Wet" samples were prepared by equilibrating films in DI water for 24 h prior to measurement. Samples were mounted between the grips of a tensile tester (MTS EM System 6430 with load frame 2208) and placed under tension at a grip separation rate of 2.54 cm (1 in.) per minute. Wet-state samples were evaluated using a custom-built chamber that was attached below the lower grip of the instrument; the chamber extended above the upper grip, and the chamber was filled with liquid DI water such that samples were completely submerged in water during the wet-state tensile experiments.

Liquid Water Permeability. Pure water permeability was measured using a dead-end cell apparatus (HP4750 Stirred Cell, Sterlitech Corp., Kent, WA) described previously.[44] Measurements were performed at ambient temperature, T, which varied from 22 to 25 °C. DI water was pressurized on one side of a porous stainless steel-supported swollen polymer film, which was approximately 28 μm (aluminum-neutralized samples) or 50 μm (non-neutralized samples) thick. The downstream side of the membrane was maintained at ambient pressure, and the pressure difference across the film, Δp, did not exceed 800 psi (55.2 bar). Polymer film thickness, l, was measured immediately following completion of the pure water permeability experiment[44] using a Litematic VL-50A (Mitutoyo, Aurora, IL) micrometer. Multiple thickness measurements were made on each sample, and the thickness variability for each sample was typically around 5%. The steady state permeate flux, n_w, was measured over a time period ranging from several hours to days, and water permeability was calculated using the classical equation from a simplified theory of reverse osmosis,[58,60] i.e.

$$P_w = \frac{n_w l R T}{\overline{V}_w[\Delta p - \Delta \pi]} \tag{6}$$

where R is the gas constant, $\overline{V}_w$ is the molar volume of water (18 cm^3 mol^{-1}),[61] and $\Delta\pi$ is the osmotic pressure difference, which was zero for pure water permeability measurements, across the film. The apparent, concentration averaged water diffusion coefficient, D_w, was calculated from the permeability coefficient and water sorption coefficient using eq 5.

Water Vapor Transmission Rate. Water vapor transmission rate (WVTR) was measured using an inverted-cup technique that has been previously described.[39] The experimental procedure followed ASTM E 96[62] except that the cup size and air flow specifications were optimized because the materials considered in this study exhibit high WVTR. Glass vials were filled with DI water and the polymer film samples, which were nominally the same thickness as those used in the liquid water permeability experiments, were used as septa. The vials were inverted such that liquid water contacted the upstream side of the polymer film, and the vials were placed in a controlled humidity/temperature environmental chamber at 23 °C and 50% relative humidity. A fan was used to reduce the water vapor boundary layer at the downstream face of the film. WVTR, reported as mass flux, was measured by measuring the mass of the sealed vial over time.

Salt Permeability. Salt permeability was measured at 25 °C and atmospheric pressure using a glass diffusion cell apparatus (PermeGear, Hellertown, PA) that has been described in the literature.[44] The polymer film thickness was nominally equivalent to that described in the liquid water permeability experiments. Aqueous sodium chloride (NaCl) solutions ranging from 0.01 to 1.0 mol/L were placed in the diffusion cell's donor cell, while atmospherically equilibrated DI water was placed in the receiver cell. The conductivity of the receiver solution was recorded as a function of time using a WTW Inolab Cond 730 Conductivity meter (Weilheim, Germany) equipped with a WTW LR 325/01 Conductivity Measuring Cell (cell constant = 0.1 cm^{-1}) (Weilheim, Germany). Using a standard calibration curve, the concentration of NaCl in the receiver solution was deduced from the conductivity measurements. The salt permeability, P_s, was calculated by fitting the conductivity data to the following equation, derived from a transient mass balance on the receiver cell[63]

$$\ln\left[1 - \frac{2C_{sl}^s[t]}{C_{s0}^s[0]}\right] = -\left(\frac{2AP_s}{Vl}\right)t \tag{7}$$

where A is the diffusion cell area available for salt transport (1.77 cm^2), V is the receiver and donor cell solution volumes (35 mL), C_{s0}^s [0] is the salt concentration in the donor cell at the beginning of the experiment (i.e., at $t = 0$), and C_{sl}^s [t] is the salt concentrations in the receiver cell at time t. Equation 7 applies for the specific case where the donor and receiver cell volumes are equal.

Like water permeability, salt permeability can be expressed as the product of salt sorption (or partition) coefficient, K_s, and the effective salt diffusion coefficient, D_s[57,58]

$$P_s = K_s D_s \tag{8}$$

Salt Sorption and Diffusion. Salt sorption was measured using a desorption method described in the literature.[13,63] Circular polymer discs were equilibrated at room temperature in a 1 mol/L sodium chloride solution, C_e, at neutral pH. The volume of the polymer sample, V_p, was determined by measuring the diameter and thickness of the swollen polymer disk, and typical values were between 0.025−0.030 cm^3. Surface moisture was quickly wiped off the sodium chloride solution-equilibrated films, and they were subsequently immersed in DI water. The sorbed sodium chloride was allowed to desorb from the polymer film over a time period that was at least 20 times l^2/P_s, which should be an overestimate of the characteristic time to reach diffusional steady state transport of salt through the polymer film.[64] The volume of DI water used for the desorption step, V_d, was chosen, using an iterative approach, such that the concentration of salt in the solution at the end of the desorption, C_d, would be approximately 1 mg(NaCl)/L because this concentration balances the desire to have a low concentration of salt in the desorption solution (i.e., to maximize salt extraction from the polymer) and the need to have a salt concentration that can be accurately quantified. The salt concentration in the desorption solution was measured using ion chromatography (ICS-2100, Dionex Corp., Sunnyvale, CA). The salt sorption coefficient was calculated as follows

$$K_s = \frac{C_d V_d}{C_e V_p}[=]\frac{g_{\text{salt}}/cm^3_{\text{swollen polymer}}}{g_{\text{salt}}/cm^3_{\text{solution}}} \tag{9}$$

dx.doi.org/10.1021/ie202546z | Ind. Eng. Chem. Res. 2013, 52, 1056−1068

The apparent salt diffusion coefficient was calculated from the measured salt permeability and sorption coefficient using the solution diffusion model[57]

$$D_s = \frac{P_s}{K_s} \tag{10}$$

Positron Annihilation Lifetime Spectroscopy (PALS). Positron annihilation lifetime spectroscopy measurements were made at room temperature on dry and DI water-equilibrated samples. 'Dry' samples were measured in a 50% relative humidity atmosphere; the samples were allowed to equilibrate in this atmosphere prior to the experiment. Wet samples were prepared by rinsing and equilibrating films in DI water for 24 h prior to the experiment.[44] Wet samples were maintained in a sealed chamber filled with DI water during the PALS experiment.

The positron source for the experiment was $^{22}NaCl$ that was sealed in a water-tight Mylar envelope. This source was placed between two polymer film stacks that were approximately 1 mm thick; the samples were stacked to this thickness to ensure that essentially all of the positrons generated by the source would annihilate within the polymer sample.[65,66] The sample-source-sample stacks were enclosed in aluminum foil to eliminate electrical interference resulting from ionization of the polymer. An automated EG&G Ortec fast−fast coincidence system was used to collect PALS data; the system measured 60,000 peak counts with a timing resolution of 217 ns. At least three spectra were taken for each sample.

A computer program, LT (version 9.0), was used to deconvolute the spectra into lifetime and intensity data for three components.[67] The lifetime of the first component, attributed to *para*-positronium, was fixed to 125 ps, but all other PALS parameters were allowed to vary.[65,68,69] The first and second components, which were attributed to *para*-positronium and free positron annihilation, respectively, were not considered beyond the fitting calculations. The third component was attributed to *ortho*-positronium (o-Ps) annihilation in free volume cavities in the sample; free volume information is often inferred from o-Ps lifetime, τ_3, data.[14,65,68−79]

A fourth o-Ps component was considered to account for the positron signature of water in the DI water-equilibrated samples. As has been observed in other systems, the intensity of this water contribution was negligible compared to the material's PALS signature.[69,80] Additionally, the contribution of the Mylar envelope was measured by running the PALS experiment on aluminum metal standards. The Mylar envelope's intensity component was negligible compared to the results obtained in the polymer sample experiments. Therefore, neither a fourth component nor a source correction factor was applied in this study.

Free volume information was obtained from the o-Ps lifetime data using the Tao-Eldrup model to relate the o-Ps lifetime to the average radius, r, of a free volume element[65,68,81,82]

$$\tau_3 = \frac{1}{2}\left(1 - \frac{r}{r + \Delta r} + \frac{1}{2\pi}\sin\left[\frac{2\pi r}{r + \Delta r}\right]\right)^{-1} \tag{11}$$

where Δr is the empirical electron layer thickness (1.66 Å).[65] Since the polymers of interest in this study are sulfonated, electron withdrawing moieties, such as sulfonate groups, can inhibit the formation of o-Ps; this interaction between positrons and sulfonated polymers can result in o-Ps intensity values that are not representative of free volume element concentrations in the polymer.[14,65,78,83] We consider the o-Ps lifetime to be representative of the average polymer free volume element size,[14] and as it may be useful to other researchers, we report the o-Ps intensity data with limited discussion.

RESULTS AND DISCUSSION

Solid State NMR. The ^{27}Al magic angle spinning (MAS) NMR spectrum of the aluminum neutralized sample is shown in Figure 3; the spectrum confirms that aluminum is present in the polymer matrix. A single, slightly asymmetric, line with a peak shift of 0.1 ppm was observed, indicating that the aluminum atoms were octahedrally coordinated with oxygen.[84] The small peaks located above and below 100 and −100 ppm are spinning sidebands.[85] The line asymmetry indicates a degree of variation in the AlO_6 coordination geometry. The octahedral coordination of the aluminum atoms in the polymer can be understood by considering the three Al−O bonds suggested in Figure 2, and the additional three coordination sites can likely be attributed to either the sulfonate group's double-bonded oxygen atoms or absorbed water.

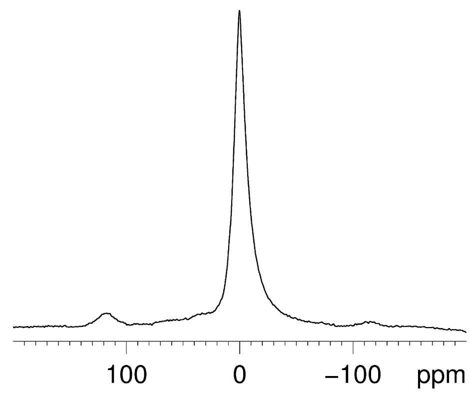

Figure 3. ^{27}Al MAS NMR spectrum for the aluminum-neutralized sulfonated pentablock copolymer.

Small Angle X-ray Scattering. Both non-neutralized and aluminum neutralized polymer films exhibited a primary SAXS peak, but the absence of higher-angle SAXS peaks indicates that the materials do not exhibit discernible long-range order. The primary spacings in wet and dry films of the non- and aluminum-neutralized polymers were determined from SAXS data. The primary spacing is a measure of the size scale of the morphology in these microphase separated block copolymers. The data, Table 1, show that both water content and the aluminum-neutralization process affect the material's morphology.

The primary spacing of the polymer decreases upon aluminum neutralization, as is apparent from the dry film SAXS data. This observation is consistent with structural

Table 1. Primary Spacing As Measured by SAXS for Non-Neutralized and Aluminum-Neutralized Sulfonated Pentablock Copolymers

	primary spacing [nm]	
sample	dry (0% RH) films	wet films
non-neutralized	30.0	46.4
aluminum-neutralized	25.0	25.2

Table 2. Liquid Water Uptake, Effective Water Diffusion Coefficient, and Liquid Water Permeability Data for Aluminum-Neutralized and Non-Neutralized Sulfonated Pentablock Copolymers[44]

sample	water uptake [g(H_2O)/g(dry polymer)]	K_w	D_w [cm^2/s]	P_w [cm^2/s]
non-neutralized	1.286 ± 0.11	0.562 ± 0.022	1.41×10^{-4}	7.91×10^{-5}
aluminum-neutralized	0.233 ± 0.007	0.189 ± 0.004	2.41×10^{-6}	4.56×10^{-7}

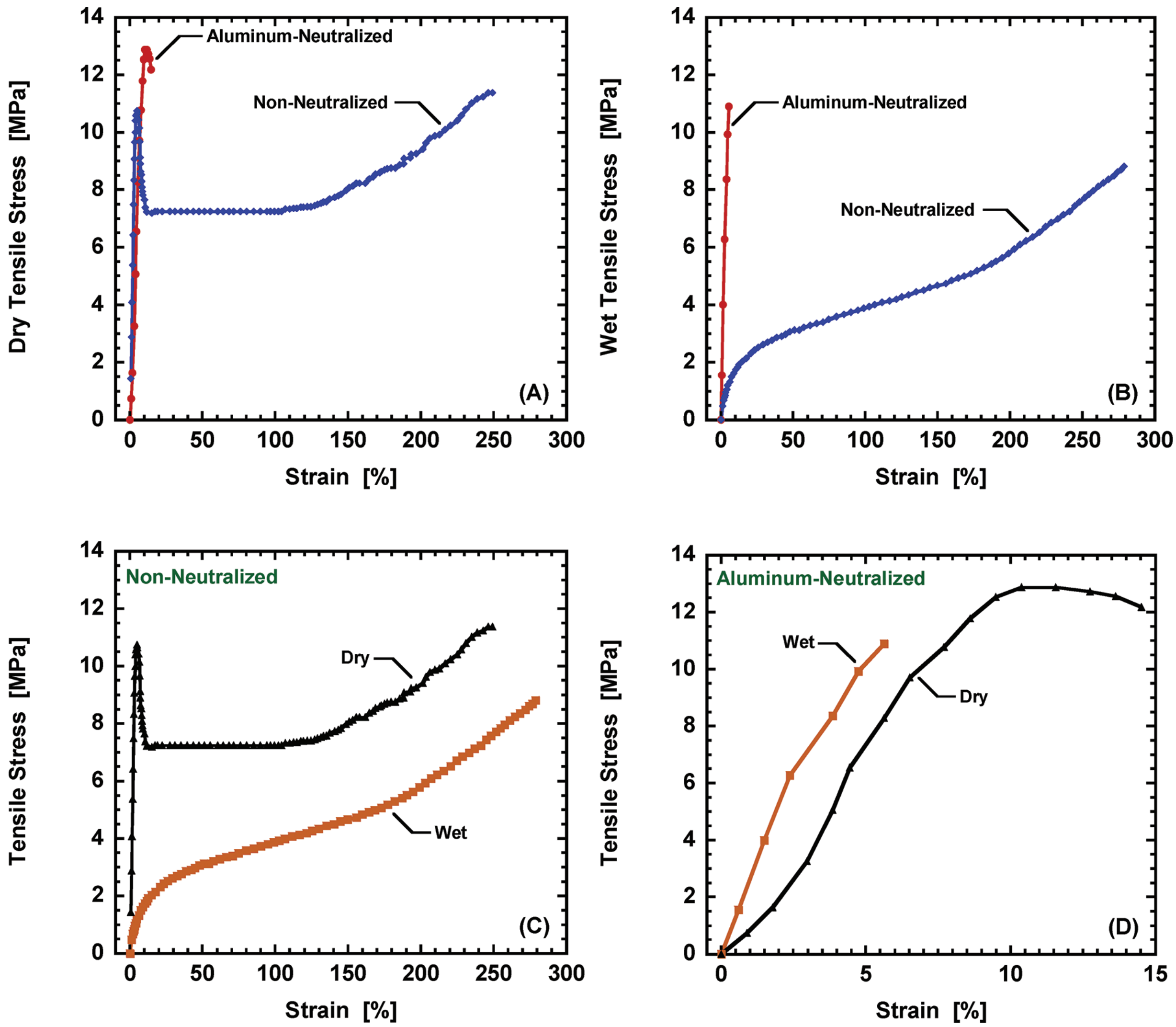

Figure 4. Tensile stress−strain curves for aluminum-neutralized and non-neutralized sulfonated pentablock copolymers. In these experiments, "dry" refers to measurements performed while the films were exposed to laboratory conditions (nominally 50% RH).

densification expected upon cross-linking. The SAXS results, however, also indicate that water-induced swelling affects the primary spacing; water swollen films tend to have larger primary spacings. The larger difference between primary spacings in the dry and wet non-neutralized samples compared to the aluminum-neutralized samples is likely due to a combination of cross-linking and lower water swelling, as will be discussed later.

Aluminum Leaching Experiment. The aluminum concentration analysis of the salt solution revealed that 0.115 ± 0.002 meq/g(dry polymer) of aluminum, which is approximately 5% of the aluminum required to completely neutralize the polymer's sulfonic acid functionality, desorbed from the polymer matrix during 2 days of soaking in the 1 mol/L sodium chloride solution. Since an excess of triethylaluminum, on an equivalent basis, was used to neutralize the polymer, we attribute this small amount of aluminum leaching to excess aluminum, which remained in the polymer matrix following the initial DI water soaking step.

To further test the polymer's resistance to ion exchange to the sodium counterion form, the same polymer samples were subsequently soaked in a second excess volume of 1 mol/L NaCl. After 30 days of soaking, the aluminum desorption was 0.020 ± 0.0002 meq/g(dry polymer), which is less than 1% of the aluminum required to completely neutralize the polymer's sulfonic acid functionality. This small amount of aluminum is most likely the remainder of the excess aluminum escaping from the polymer matrix.

Following the leaching experiment, the polymer film samples were ashed in a furnace at 700 °C to burn off the organic components of the polymer. The resulting white ash was not soluble in either DI water or 2% nitric acid, suggesting that it may be composed of aluminum oxide material.[37] Based on these experimental results, the aluminum-sulfonate group bonds in the polymer appear to be resistant to ion exchange, at least by NaCl.

Water Uptake. The water uptake of the aluminum-neutralized polymer was measured and compared to that of the non-neutralized polymer to probe the effect of aluminum neutralization on the polymer's hydrophilicity. The pure water uptake values for both materials are shown in Table 2. Aluminum neutralization results in a 5.5-fold decrease in water uptake. This decrease is consistent with neutralization of a highly charged functional group[19] and polymer cross-linking, both of which should limit material swelling.[24,28] Additionally, the lower water uptake of the aluminum-neutralized polymer compared to that of the non-neutralized polymer is reflected in the SAXS primary spacing data shown in Table 1; the large difference in SAXS primary spacing of the non-neutralized material is characteristic of a material that swells to a considerable degree.

Water uptake was also measured when the polymer film samples were soaked in 1 mol/L NaCl solution. The water uptake of the non-neutralized sulfonated pentablock copolymer decreases when the material is soaked in 1 mol/L NaCl. This decrease occurs, in part, because the salt in the solution depresses the activity of water in the solution,[86] but other effects, such as decreased water uptake that results from the acid to sodium form ion exchange process,[87] may also contribute. The water uptake values for the non-neutralized and aluminum-neutralized sulfonated pentablock copolymers in 1 mol/L NaCl are 0.519 ± 0.009 and 0.231 ± 0.006 g(H_2O)/g(dry polymer), respectively. The decrease in water content of the aluminum-neutralized polymer soaked in 1 mol/L NaCl was negligible compared to the pure water uptake value. Furthermore, the water uptake of the aluminum-neutralized film did not increase after returning the 1 mol/L NaCl solution-equilibrated films to soak in DI water. The difference in the swelling behavior as a function of salt concentration of the two materials is likely due to the reduced hydrophilicity of the aluminum-neutralized polymer; solvent uptake in less hydrophilic polymers will be less sensitive to changes in solvent activity than that of more hydrophilic polymers.[88]

The water uptake and dimensional stability, characterized by the diameter of a polymer disk, of the aluminum-neutralized polymer were measured over a five week period. During this experiment, the polymers were stored in DI water. The water uptake and the diameter of the polymer discs remained constant over the five week period. Thus, the aluminum-neutralized polymers appear to be stable in DI water.

Tensile Experiments. *Dry Materials.* The stress−strain curves for the sulfonated pentablock copolymer prior to aluminum neutralization tested "dry", as defined earlier, is shown in both Figure 4A and C. After experiencing a sharp postyield relaxation, the material strain hardens until failure at roughly 250% elongation. The material's toughness is attributed to the copolymer's hydrogenated isoprene blocks and to some degree of plasticization of the sulfonated styrene domain by water sorbed from the laboratory atmosphere. The tensile stress−strain curve for the "dry" polymer after aluminum neutralization is shown in both Figure 4A and D. Aluminum neutralization modestly increases the polymer's stress at yield but makes the material more brittle than the non-neutralized polymer.

Wet Materials. Tensile stress−strain curves in the "wet" state are shown for both the non-neutralized and aluminum-neutralized polymers in Figure 4B, C, and D. Hydration of the non-neutralized polymer (Figure 4C) results in a swollen polymer that is very ductile and has essentially no yield event. The aluminum-neutralized polymer remains strong in the wet-state. The observation, in Figure 4D, that the aluminum-neutralized polymer is more ductile in the "dry" state than the "wet" state polymer might be understood by considering the swollen nature of the wet-state polymer compared to the dry-state polymer; swelling of the sulfonated domains impose a deformation of the polymer chains that might limit their subsequent extensibility under stress. Of course, these are complex multiphase materials, and other factors may also contribute.

Water and Salt Transport. Small molecule transport in nonporous polymers can be described by the solution-diffusion model.[4,7,57,58] The transport of small molecules occurs by molecular diffusion and can be an effective probe of molecular structure. Water and salt transport properties of the aluminum-neutralized polymer were studied to indirectly probe the effect of aluminum neutralization on the polymer structure.

Water Permeability and Water Vapor Transport Rate. Water transport is an important property for several applications such as membrane-based dehydration (e.g., energy recovery ventilation (ERV)), forward osmosis, pressure-retarded osmosis, and desalination.[4,7,89−95] Two different water transport experiments, hydraulic water permeability and water vapor transport rate, were employed to study water transport through the non-neutralized and aluminum-neutralized polymers. These two experiments expose the membrane to different hydration conditions, which may influence the polymer's morphology and, in turn, transport properties.

The equations used to calculate water permeability (eq 6) and the apparent water diffusion coefficient (eq 5) are the classic reverse osmosis equations that apply to homogeneous materials that sorb relatively little water.[58] The materials considered here are phase-separated, and thus, heterogeneous, and at the present time, insufficient morphological information is available to interpret the permeability and diffusion coefficient values in light of the material's heterogeneity. Furthermore, the non-neutralized polymer sorbs a considerable amount of water, and the simple model applied here does not explicitly separate convective frame of reference terms from diffusion, and such convective effects become more important as swelling increases.[58,96−98] Consequently, the apparent water diffusion coefficient reported for the non-neutralized polymer is physically unrealistic; indeed, the value in Table 2 exceeds the self-diffusion coefficient of water (2.8×10^{-5} cm^2 s^{-1}).[96] Appropriate models, as reported in the literature,[58,96,99] can be used to separate the convective effects from diffusion *per se* to yield diffusion coefficients that are well below the self-diffusion coefficient of water. Analysis of the current data in terms of these models, however, is beyond the scope of the present work, and thus, the reported water permeability and diffusion coefficient data should be understood to be effective (or apparent) values.

Water permeability, P_w, and apparent water diffusion coefficient, D_w, data are recorded in Table 2. Both the water permeability and diffusion coefficients decrease by roughly 2 orders of magnitude upon aluminum neutralization; this decrease is likely the result of two inter-related factors: reduced swelling and cross-linking. Polymer water content plays a

dx.doi.org/10.1021/ie202546z | Ind. Eng. Chem. Res. 2013, 52, 1056−1068

significant role in determining water transport as can be seen from the relationship between P_w and K_w in eq 5. There is, however, an indirect influence of water content on water transport; water sorption plasticizes the polymer matrix, thereby causing the apparent diffusion coefficient to increase, possibly strongly, with increasing water content.[44] To put the water permeability values in perspective, if the non-neutralized and aluminum neutralized polymers were prepared as 100 nm thick films, which is comparable to commercial desalination membranes, the water flux through those hypothetical films, with a 15.5 bar hydrostatic pressure difference applied, would be 3210 and 1.4 L m^{-2} hr^{-1}, respectively; these values can be compared to the water flux, 45 L m^{-2} hr^{-1}, of a commercially available brackish water RO membrane (DOW BW30-400) under similar conditions.[100]

Yasuda et al.'s free volume-based model suggests that transport of water, salts, and other water-soluble species occurs only in hydrated regions of the polymer; they assumed that the free volume, v_f, of those hydrated regions scales linearly with water content, i.e., $v_f \sim K_w$.[63,101] Recent studies, using PALS, suggest that this scaling is obeyed in uncharged hydrogels as well as random copolymers based on sulfonated polysulfone.[14,71] From free volume theory, the diffusion coefficient, D, should scale as follows

$$D \propto \exp\left[-\frac{v^*}{v_f}\right] \tag{12}$$

where v^* is the minimum characteristic free volume element size required to permit the diffusing penetrant to execute a diffusion step.[63,102] Therefore, $\log[D_w]$ is expected to scale with $1/K_w$.[63] The sorption component, K, of the solution-diffusion model for permeability, P, is typically less sensitive to free volume than the diffusion coefficient, so $\log[P_w]$ often also scales with $1/K_w$.[7,63]

Figure 5 presents a plot of $\log[P_w]$ versus $1/K_w$ for the aluminum-neutralized polymer and non-neutralized sulfonated pentablock copolymers of varying degrees of sulfonation.[44] Based upon this figure, the reduction in water uptake that accompanies aluminum neutralization and the effect of that water content change on the polymer's apparent water diffusion coefficient are primarily responsible for the observed decrease in water permeability. Therefore, changes in water sorption resulting from sulfonate group neutralization are likely responsible for the observed decrease in water permeability, via the reduced free volume that accompanies lower water sorption.

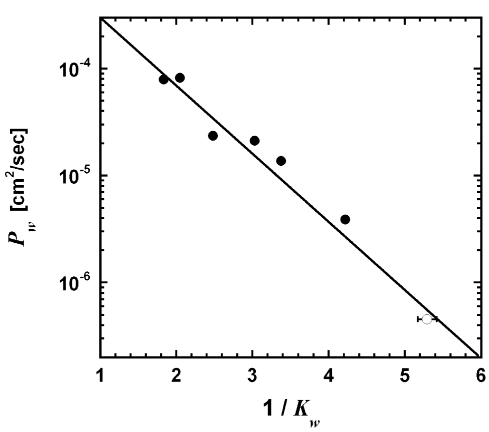

Figure 5. Water permeability scales with $1/K_w$, as expected from free-volume theory, for aluminum-neutralized (○), and non-neutralized sulfonated block copolymers (●).[44]

Furthermore, cross-linked polymers generally exhibit reduced permeability and diffusion coefficients, relative to their uncross-linked analogs, because cross-links can restrict polymer segmental motion.[103−105] Chain motion is a necessary component of the solid-state diffusion process by which small molecules move through the polymer. While cross-linking may contribute to the observed decrease in water permeability, this effect is likely secondary to the decrease in water sorption caused by the neutralization process.

Water vapor transport rate was also affected by aluminum neutralization. The WVTR decreased from 24 to 22 kg m^{-2} day^{-1} upon aluminum neutralization. WVTRs of 24 and 22 kg m^{-2} day^{-1} correspond to water permeability values of 1.0×10^{-7} and 9.2×10^{-8} cm^2 s^{-1}, respectively, for a 25 μm thick film when the downstream face of the film is assumed to be equilibrated at a water activity value of 0.5 (50% relative humidity) and boundary layer effects, which would have the effect of decreasing permeability, are neglected. This low water permeability is understandable considering that the WVTR experiment exposes the downstream side of the polymer film to air at 50% relative humidity. In contrast, the application of 800 psi (55.2 bar) feed pressure in the hydraulic water permeability experiment is equivalent to exposing the downstream face of the membrane to air at 96% humidity, so that the overall concentration of water in the sample used for hydraulic permeability should be much higher than that in the sample used for WVTR measurements.[58] Even though the driving force for mass transfer is greater in the WVTR experiment, the water content at the downstream side of the film is considerably lower in the WVTR experiment than in the hydraulic permeability experiment because the activity of water in equilibrium with the downstream side of the film is lower in the WVTR experiment compared to the hydraulic permeability experiment. Given the sensitivity of polymer morphology (Table 1) and water permeability (Figure 5) to water content, less water transport would be expected in the WVTR experiment compared to the hydraulic permeability experiment. Since the morphology of these materials is sensitive to water content, morphology-limited water transport may also explain the difference in water transport between the WVTR and hydraulic permeability experiments. The relatively small difference in WVTR between the aluminum-neutralized and non-neutralized polymers may be related to the water content of the materials. At the low water content experienced at the downstream side of the film in the WVTR experiment, the morphological and diffusive restrictions to mass transfer may overshadow the effects of aluminum neutralization.

Salt Permeability, Sorption, and Diffusion. Polymer salt permeability decreases upon aluminum neutralization. This result is expected and can be understood considering the above discussion on the decrease in water permeability upon aluminum neutralization. Different behavior, however, is observed upon neutralization when salt permeability is studied as a function of upstream salt concentration.

The salt permeability of highly charged polymers, such as sulfonated polymers, is expected to increase as the upstream salt concentration increases according to Donnan theory.[4,44,106] This increase in salt permeability is believed to be a result of increased salt sorption as Donnan exclusion becomes less effective at higher salt concentrations.[2,4] In contrast, non-charged polymers, such as poly(ethylene glycol) and cellulose acetate, typically have salt permeabilities that are much less sensitive to salt concentration.[60,107,108]

Figure 6 presents salt permeability data for the polymers as a function of upstream (donor cell) salt concentration. The salt

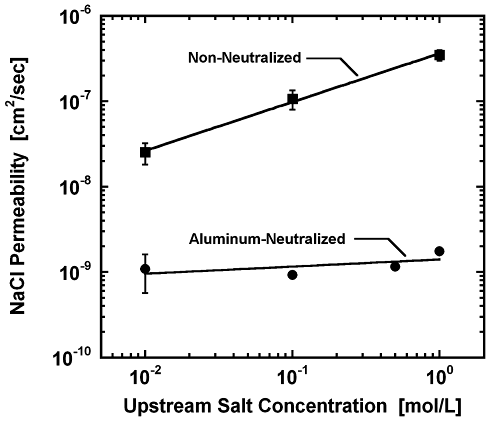

Figure 6. Aluminum- and non-neutralized[44] polymer salt permeability versus upstream (donor cell) salt concentration.

permeability of the aluminum-neutralized polymer is less sensitive to upstream salt concentration compared to the non-neutralized polymer. According to Donnan theory, this observation suggests that the aluminum-neutralized polymer has a lower effective fixed charge density than the non-neutralized polymer.[4] This result further suggests that the aluminum neutralization process is successful and that the aluminum-sulfonate group bonds are more stable and covalent in nature than the proton- and sodium-sulfonate group bonds. Thus, aluminum neutralization is an effective way to reduce both the salt permeability of a sulfonated pentablock copolymer and the sulfonated polymer's salt permeability dependence on upstream concentration.

Salt sorption measurements (Table 3) show that the salt sorption coefficient decreases upon aluminum-neutralization of

Table 3. Salt Permeability, Sorption Coefficient, and Apparent Diffusion Coefficient for Non- and Aluminum-Neutralized Polymers (All Measurements Taken at 1 mol/L NaCl)

sample	P_s [cm^2/s]	K_s	D_s [cm^2/s]
non-neutralized	3.49×10^{-7}	0.155 ± 0.016	2.25×10^{-6}
aluminum-neutralized	1.76×10^{-9}	0.089 ± 0.001	1.98×10^{-8}

the polymer. Based on Donnan exclusion, the decrease in the salt sorption coefficient upon aluminum neutralization may seem unexpected. The sample's water uptake, however, is a key factor in determining the salt sorption coefficient. Generally, the salt sorption coefficient increases as water uptake increases;[13,60,71,103] as the polymer becomes more swollen, it is able to absorb additional salt. Therefore, the decrease in water uptake that results from aluminum-neutralization of the sulfonated pentablock copolymer causes the salt sorption coefficient to decrease even though the polymer's charged functionality is neutralized during the process, which would tend to favor increased salt sorption.

The apparent salt diffusion coefficient decreases upon aluminum-neutralization, and this result is likely due mainly to the decrease in water uptake that occurs upon neutralization as was discussed in regard to the decrease in the apparent water diffusion coefficient upon neutralization. A plot of log[P_s] versus $1/K_w$ is shown as Figure 7 to illustrate the effect of water

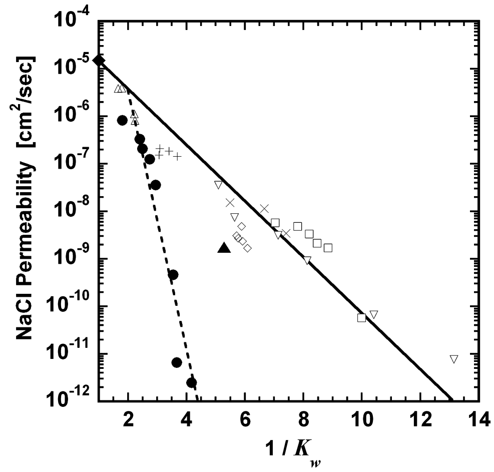

Figure 7. Sodium chloride permeability plotted versus $1/K_w$ for the materials listed in the legend (Table 4). The aluminum-neutralized polymer is represented by the symbol: ▲.

content on salt permeability. The solid line in Figure 7 is the empirical correlation between hydrogel salt permeability and water content for a series of hydrogels as reported by Yasuda et al.[63] The dashed line is the empirical correlation reported for the non-neutralized sulfonated pentablock copolymers prepared with different degrees of sulfonation.[44] The data point for the aluminum-neutralized polymer falls closer to the correlation for uncharged materials. This result is consistent with the observation in Figure 6 that the aluminum-neutralized polymer's salt permeability is less sensitive to salt concentration as a result of the neutralization of the material's sulfonate groups. The data in Figure 7 further suggest that the aluminum-sulfonate group bonds are stable and the aluminum-neutralized polymer is effectively less highly charged than the non-neutralized polymer as a result of the aluminum neutralization process.

Water/Salt Selectivity. Permeability, diffusion, and sorption selectivity values can be defined using the solution diffusion model.[7] The permeability selectivity, P_w/P_s, indicates the degree to which water permeates through the polymer film relative to salt. The diffusion selectivity, D_w/D_s, and sorption selectivity, K_w/K_s, indicate the degree to which water preferentially diffuses

Table 4. Legend for Figure 7

symbol	sample
▲	aluminum-neutralized pentablock copolymer
●	non-neutralized pentablock copolymers[44]
▽	methyl methacrylate/glycerol methacrylate copolymer[63]
□	hydroxypropyl methacrylate/methyl methacrylate copolymer[63]
◇	hydroxypropyl methacrylate/glycidyl methacrylate copolymer[63]
×	hydroxyethyl methacrylate/methyl methacrylate copolymer[63]
+	hydroxyethyl methacrylate hydrogel[63]
Δ	hydroxyethyl methacrylate/glycerol methacrylate hydrogel[63]
◆	NaCl diffusion coefficient in water at 25 °C (1.5×10^{-5} cm^2 s^{-1})[109]

dx.doi.org/10.1021/ie202546z | Ind. Eng. Chem. Res. 2013, 52, 1056−1068

through or sorbs into the polymer matrix relative to salt. The values for the aluminum-neutralized and non-neutralized polymer's permeability, diffusion, and sorption selectivities are shown in Table 5. To put these values in perspective, a commercial brackish water RO membrane (DOW BW30-400) has a permeability selectivity (P_w/P_s) of approximately 19,800, which is equivalent to a salt rejection of 99.5% when the membrane is operated with a feed of 2,000 mg (NaCl)/L at 25 °C, a transmembrane pressure difference of 15.5 bar, and a recovery of 15%.[100] Due to the interfacial polyamide polymerization process used to prepare the BW30-400 membrane, it is not possible to split the permeability selectivity into its diffusivity and sorption selectivity components.

Table 5. Permeability, Diffusion, and Sorption Water/Salt Selectivity (Salt: 1 mol/L NaCl)

sample	P_w/P_s	D_w/D_s	K_w/K_s
non-neutralized	227	63	3.6
aluminum-neutralized	259	122	2.1

The increase in permeability selectivity upon aluminum neutralization is due to an increase in diffusion selectivity. The aluminum-neutralized polymer's larger diffusion selectivity compared to that of the non-neutralized polymer is likely due to the lower water content of the aluminum-neutralized polymer compared to the non-neutralized polymer and aluminum cross-linking. Cross-linking generally increases a polymer's diffusion and permeability selectivity, which would tend to result in an increase in salt rejection.[104,105] Sorption selectivity decreases upon aluminum neutralization; this result is likely due to decreased Donnan exclusion that results from fixed charge neutralization.[2,4]

Positron Annihilation Lifetime Spectroscopy Analysis of Free Volume. Polymer free volume was measured using positron annihilation lifetime spectroscopy. The size, presented as a spherical radius, of the polymer's free volume elements correspond to the efficiency of chain packing in the polymer matrix.[65,68] Furthermore, free volume has been shown to be related to a variety of polymer properties including small molecule transport, viscosity, glass transition temperature, and molecular weight.[65]

The pentablock copolymers studied here are multiphase materials. PALS measures the average o-Ps lifetime and intensity over an entire sample, so contributions from the *t*-butylstyrene and hydrogenated isoprene blocks are present in the reported PALS data. The standard deviations of the o-Ps lifetimes and intensities were typically less than 1% of the average values, which indicates that it is appropriate to analyze the data as a monomodal o-Ps lifetime distribution. Furthermore, both the aluminum- and non-neutralized pentablock copolymers were derived from the same block copolymer, so the subsequent PALS analysis illustrates changes in the material that result from neutralization of the polymer's hydrophilic domain because the contributions from the hydrophobic blocks are presumably the same in both materials.

In the dry-state, the o-Ps lifetime, τ_3, decreases upon aluminum neutralization as seen in Table 6. This result suggests that the aluminum cross-linking that occurs during the neutralization process acts to improve polymer chain packing. This improved chain packing can be observed as a decrease in the average free volume element (FVE) radius upon neutralization. This result is consistent with the observed increase in polymer density upon aluminum neutralization.

Table 6. PALS Results for Aluminum-Neutralized and Non-Neutralized Polymers in Different Experimental Environments

environment	sample	τ_3 [ns]	FVE radius [Å]	I_3 [%]
dry (50% RH)	non-neutralized	2.14 ± 0.02	2.98 ± 0.02	14.6 ± 0.2
	aluminum-neutralized	2.01 ± 0.02	2.87 ± 0.01	17.1 ± 0.1
wet-state	non-neutralized	1.98 ± 0.01	2.84 ± 0.01	19.2 ± 0.1
	aluminum-neutralized	1.96 ± 0.01	2.82 ± 0.01	20.5 ± 0.2

In the wet-state, no statistical difference in τ_3 was observed upon aluminum neutralization. However, the analysis of the wet-state results must include consideration for the water uptake of the materials. While the intensity of a discrete water component was negligible in the PALS experiment, absorbed water will affect the PALS results for the swollen polymer system.[14,71] The o-Ps lifetime of liquid water is 1.86 ± 0.02 ns;[110] therefore, increases in water sorption are expected to decrease τ_3 for the swollen polymer system.[14] Since the non-neutralized material sorbs considerably more water than the aluminum-neutralized material (Table 2), the non-neutralized polymer's τ_3 may be more depressed by water sorption than that for the aluminum-neutralized polymer.

A non-neutralized sulfonated pentablock copolymer with an ion exchange capacity (IEC) of 0.7 meq/g(dry polymer) has an identical water uptake (0.233 g(H_2O)/g(dry polymer))[44] to that of an aluminum-neutralized IEC 2.0 sulfonated pentablock copolymer. While comparison of these two materials neglects the lower concentration of sulfonate groups in the IEC 0.7 polymer compared to the neutralized IEC 2.0 polymer, comparison at similar water uptake is useful for the analysis of the PALS data. The wet-state IEC 0.7 polymer o-Ps lifetime is 2.03 ± 0.01 ns. When this value is compared to the wet-state aluminum-neutralized o-Ps lifetime (1.96 ± 0.01 ns), the result is found to be the same as was observed in the dry-state; o-Ps lifetime decreases upon aluminum neutralization.

■ CONCLUSIONS

An acid-form sulfonated styrenic pentablock copolymer was neutralized in suspension using excess triethylaluminum. Aluminum neutralization was confirmed by ^{27}Al solid state NMR, and the aluminum-sulfonate group bonds were found to resist ion exchange to the sodium counterion form. Based upon the trivalent nature of aluminum, aluminum neutralization may cross-link the polymer. The primary spacing, as measured by SAXS, decreased upon aluminum neutralization, and the primary feature spacing increased as the polymer sorbed water. The polymer's free volume element size decreased upon aluminum neutralization, and the free volume element size depends on water uptake.

The aluminum neutralization process influences the material's mechanical properties. Aluminum neutralization produced a stronger hydrated polymer compared to the hydrated non-neutralized polymer. The dry aluminum-neutralized polymer was more brittle than the non-neutralized polymer.

dx.doi.org/10.1021/ie202546z | Ind. Eng. Chem. Res. 2013, 52, 1056−1068

Water and sodium chloride transport properties were affected by the aluminum neutralization process. Aluminum neutralization of the polymer's sulfonate groups resulted in a 5.5-fold decrease in water uptake. Consequently, the aluminum-neutralized polymer's water and salt permeability and water vapor transport rate decreased. An additional effect of the aluminum neutralization process was a decrease in the sensitivity of sodium chloride permeability to salt concentration. This result is consistent with Donnan exclusion theory because neutralization of the polymer's fixed charge is expected to reduce the dependence of salt permeability on salt concentration. Also consistent with Donnan exclusion theory was the observed decrease in the water/salt solubility selectivity that was observed upon the aluminum neutralization process. Ultimately, the polymer's water/salt permeability selectivity increased upon aluminum neutralization because of a 1.8-fold increase in the water/salt diffusion selectivity. Therefore, aluminum-neutralization is an interesting strategy for tuning the morphology, mechanical properties, water and salt transport properties, and free volume of a sulfonated polymer.

AUTHOR INFORMATION

Corresponding Author

*Phone: +1-512-471-5392. Fax: +1-512-471-0542. E-mail: drp@che.utexas.edu.

Notes

The authors declare no competing financial interest.

REFERENCES

(1) Xu, T. W. Ion exchange membranes: State of their development and perspective. *J. Membr. Sci.* **2005**, *263* (1−2), 1−29.

(2) Helfferich, F. *Ion exchange*; Dover Publications: New York, 1995.

(3) Strathmann, H. Ion exchange membranes. In *Membrane Handbook*; Winston, Ho, W. S., Sirkar, K. K., Eds.; Van Nostrand Reinhold: New York, 1992; pp 230−245.

(4) Geise, G. M.; Lee, H.-S.; Miller, D. J.; Freeman, B. D.; McGrath, J. E.; Paul, D. R. Water purification by membranes: The role of polymer science. *J. Polym. Sci. Part B: Polym. Phys.* **2010**, *48* (15), 1685−1718.

(5) Mauritz, K. A.; Moore, R. B. State of understanding of Nafion. *Chem. Rev.* **2004**, *104* (10), 4535−4585.

(6) Robeson, L. M.; Hwu, H. H.; McGrath, J. E. Upper bound relationship for proton exchange membranes: Empirical relationship and relevance of phase separated blends. *J. Membr. Sci.* **2007**, *302*, 70−77.

(7) Geise, G. M.; Park, H. B.; Sagle, A. C.; Freeman, B. D.; McGrath, J. E. Water permeability and water/salt selectivity tradeoff in polymers for desalination. *J. Membr. Sci.* **2010**, *369* (1−2), 130−138.

(8) Długołecki, P.; Gambier, A.; Nijmeijer, K.; Wessling, M. Practical potential of reverse electrodialysis as process for sustainable energy generation. *Environ. Sci. Technol.* **2009**, *43*, 6888−6894.

(9) Parise, P. L.; Allegrezza Jr., A. E.; Parekh, B. S., Reverse osmosis: Chlorine-resistant polysulfone reverse osmosis membrane and module. *Ultrapure Water* **1987**, (October), 54-65.

(10) Allegrezza, A. E., Jr.; Parekh, B. S.; Parise, P. L.; Swiniarski, E. J.; White, J. L. Chlorine resistant polysulfone reverse osmosis modules. *Desalination* **1987**, *64*, 285−304.

(11) Hickner, M. A. Ion-containing polymers: New energy & clean water. *Mater. Today* **2010**, *13* (5), 34−41.

(12) Hickner, M. A.; Ghassemi, H.; Kim, Y. S.; Einsla, B. R.; McGrath, J. E. Alternative polymer systems for proton exchange membranes (PEMs). *Chem. Rev.* **2004**, *104* (10), 4587−4612.

(13) Xie, W.; Cook, J.; Park, H. B.; Freeman, B. D.; Lee, C. H.; McGrath, J. E. Fundamental salt and water transport properties in directly copolymerized disulfonated poly(arylene ether sulfone) random copolymers. *Polymer* **2011**, *52*, 2032−2043.

(14) Xie, W.; Ju, H.; Geise, G. M.; Freeman, B. D.; Mardel, J. I.; Hill, A. J.; McGrath, J. E. Effect of free volume on water and salt transport properties in directly copolymerized disulfonated poly(arylene ether sulfone) random copolymers. *Macromolecules* **2011**, *44* (11), 4428−4438.

(15) Xie, W.; Park, H. B.; Cook, J.; Lee, C. H.; Byun, G.; Freeman, B. D.; McGrath, J. E. Advances in membrane materials: Desalination membranes based on directly copolymerized disulfonated poly(arylene ether sulfone) random copolymers. *Water Sci. Technol.* **2010**, *61* (3), 619−624.

(16) Bonner, O. D.; Smith, L. L. A selectivity scale for some bivalent cations on Dowex-50. *J. Phys. Chem.* **1957**, *61*, 326−329.

(17) Suresh, G.; Pandey, A. K.; Goswami, A. Permeability of water in poly(perfluorosulfonic) acid membrane with different counterions. *J. Membr. Sci.* **2007**, *295*, 21−27.

(18) Tant, M. R.; Mauritz, K. A.; Wilkes, G. L. *Ionomers: Synthesis, structure, properties, and applications*, 1st ed.; Blackie Academic & Professional: New York, 1997.

(19) Pushpa, K. K.; Nandan, D.; Iyer, R. M. Thermodynamics of water sorption by perfluorosulphonate (Nafion-117) and polystyrene-divinylbenzene sulphonate (Dowex 50W) ion-exchange resins at 298 ± 1 K. *J. Chem. Soc., Faraday Trans. 1* **1988**, *84* (6), 2047−2056.

(20) Steck, A.; Yeager, H. L. Water sorption and cation-exchange selectivity of a perfluorosulfonate ion-exchange polymer. *Anal. Chem.* **1980**, *52* (8), 1215−1218.

(21) Weiss, R. A.; Sen, A.; Pottick, L. A.; Willis, C. L. Block copolymer ionomers: 2. Viscoelastic and mechanical properties of sulphonated poly(styrene-ethylene/butylene-styrene). *Polymer* **1991**, *32* (15), 2785−2792.

(22) Weiss, R. A.; Zhao, H. Rheological behavior of oligomeric ionomers. *J. Rheol.* **2009**, *53* (1), 191−213.

(23) Park, C. K.; Oh, B.-K.; Choi, M. J.; Lee, Y. M. Separation of benzene/cyclohexane by pervaporation through chelate poly(vinyl alcohol)/poly(allyl amine) blend membrane. *Polym. Bull.* **1994**, *33* (5), 591−598.

(24) Inui, K.; Noguchi, T.; Miyata, T.; Uragami, T. Pervaporation characteristics of methyl methacrylate−methacrylic acid copolymer membranes ionically crosslinked with metal ions for a benzene/cyclohexane mixture. *J. Appl. Polym. Sci.* **1999**, *71*, 233−241.

(25) Taubert, A.; Wind, J. D.; Paul, D. R.; Koros, W. J.; Winey, K. I. Novel polyimide ionomers: CO_2 plasticization, morphology, and ion distribution. *Polymer* **2003**, *44*, 1881−1892.

(26) Pignolet, L. H.; Waldman, A. S.; Schechinger, L.; Govindarajoo, G.; Nowick, J. S.; Ted, L. The alginate demonstration: Polymers, food science, and ion exchange. *J. Chem. Educ.* **1998**, *75* (11), 1430−1431.

(27) Wind, J. D.; Staudt-Bickel, C.; Paul, D. R.; Koros, W. J. The effects of crosslinking chemistry on CO_2 plasticization of polyimide gas separation membranes. *Ind. Eng. Chem. Res.* **2002**, *41*, 6139−6148.

(28) Matsui, S.; Paul, D. R. Pervaporation separation of aromatic/aliphatic hydrocarbons by crosslinked poly(methyl acrylate-*co*-acrylic acid) membranes. *J. Membr. Sci.* **2002**, *195*, 229−245.

(29) Tsuchida, E.; Nishide, H.; Ohyanagi, M.; Kawakami, H. Facilitated transport of molecular oxygen in the membranes of polymer-coordinated cobalt Schiff base complexes. *Macromolecules* **1987**, *20* (8), 1907−1912.

(30) Hsiue, G.-H.; Yang, J.-M. Polymeric complexed membranes used as oxygen carrier: Axial and in-plane ligand effects. *J. Polym. Sci., Part A: Polym. Chem.* **1993**, *31* (6), 1457−1466.

(31) Nishide, H.; Kawakami, H.; Sasame, Y.; Ishiwata, K.; Tsuchida, E. Facilitated transport of molecular oxygen in cobaltporphyrin/poly(1-trimethylsilyl-1-propyne) membrane. *J. Polym. Sci., Part A: Polym. Chem.* **1992**, *30* (1), 77−82.

(32) Zaikov, G. E.; Iordanskii, A. P.; Markin, V. S. *Diffusion of electrolytes in polymers*; VSP: Utrecht, The Netherlands, 1988.

(33) Paddison, S. J.; Reagor, D. W.; Zawodzinski, T. A. High frequency dielectric studies of hydrated Nafion®. *J. Electroanal. Chem.* **1998**, *459*, 91−97.

(34) Robinson, R. A.; Stokes, R. H. *Electrolyte solutions*, 2nd ed.; Dover: Mineola, NY, 2002.

(35) Vishnyakov, A.; Neimark, A. V. Specifics of solvation of sulfonated polyelectrolytes in water, dimethylmethylphosphonate, and their mixture: A molecular simulation study. *J. Chem. Phys.* **2008**, *128*, 164902−1−11.
(36) Brown, T. L.; LeMay Jr., H. E.; Bursten, B. E.; Burdge, J. R. *Chemistry: The central science*, 9th ed.; Pearson Education Inc.: Upper Saddle River, NJ, 2003.
(37) Haynes, W. M. *CRC handbook of chemistry and physics (Internet Version 2011)*, 91st ed.; CRC Press: Boca Raton, FL, 2011.
(38) Willis, C. L.; Handlin, D. L.; Trenor, S. R.; Mather, B. D. Sulfonated block copolymers, method for making same, and various uses for such block copolymers. US Patent 7,737,224 B2, June 15, 2010.
(39) Flood, J.; Dubois, D.; Willis, C. L.; Bening, R. In *Sulfonated styrenic pentablock copolymer membranes for high water transport rate applications*, ANTEC 2009 ---- Proceedings of the 67th Annual Technical Conference & Exhibition, Chicago, IL, 2009; Society of Plastics Engineers: Chicago, IL, 2009; pp 107−112.
(40) Dado, G. P.; Handlin, D. L.; Willis, C. L. Method of sulfonation of block copolymers. US Patent Application 2010/0048817 A1, Feb. 25, 2010.
(41) Willis, C. L.; Handlin, D. L.; Trenor, S. R.; Mather, B. D. Process for preparing sulfonated block copolymers and various uses for such block copolymers. US Patent Application 2010/0203784 A1, Aug. 12, 2010.
(42) Kota, A. K.; Winey, K. I. In *Morphology of sulfonated styrenic pentablock copolymer solutions and membranes*, ANTEC 2009 ---- Proceedings of the 67th Annual Technical Conference & Exhibition, Chicago, IL, 2009; Society of Plastics Engineers: Chicago, IL, 2009; pp 113−116.
(43) Geise, G. M.; Freeman, B. D.; Paul, D. R. In *Water and ion transport through sulfonated styrenic pentablock copolymer membranes for reverse osmosis applications*, ANTEC 2009 ---- Proceedings of the 67th Annual Technical Conference & Exhibition, Chicago, IL, June 22-24, 2009; Society of Plastics Engineers: Chicago, IL, 2009; pp 97−101.
(44) Geise, G. M.; Freeman, B. D.; Paul, D. R. Characterization of a novel sulfonated pentablock copolymer for desalination applications. *Polymer* **2010**, *51* (24), 5815−5822.
(45) Geise, G. M.; Freeman, B. D.; Paul, D. R., Comparison of the permeation of $MgCl_2$ versus NaCl in highly-charged sulfonated polymer membranes. In *Modern Applications in Membrane Science and Technology*; Escobar, I. C., Van der Bruggen, B., Eds.; American Chemical Society: Washington, DC, 2011; Vol. *1078*, pp 239−245.
(46) Choi, J. H.; Kota, A.; Winey, K. I. Micellar morphology in sulfonated pentablock copolymer solutions. *Ind. Eng. Chem. Res.* **2010**, *49* (23), 12093−12097.
(47) Willis, C. L. Metal-neutralized sulfonated block copolymers, process for making them and their use. US Patent Application 2011/0086977 A1, Apr. 14, 2011.
(48) Rahman, S. A.; Nemoto, N. Viscoelasticity of aluminum neutralized telechelic poly(ethylene butylene) ionomer. *J. Soc. Rheol., Jpn. (2001-2003)* **2003**, *31* (4), 219−227.
(49) Sun, L.; Thrasher, J. S. Studies of the thermal behavior of Nafion(R) membranes treated with aluminum(III). *Polym. Degrad. Stab.* **2005**, *89*, 43−49.
(50) Sivashinsky, N.; Tanny, G. B. Ionic heterogeneities in sulfonated polysulfone films. *J. Appl. Polym. Sci.* **1983**, *28*, 3235−3245.
(51) Heiney, P. A. A software tool for powder and small angle X-ray diffraction analysis. *Comm. Powder Diffr. Newsletter* **2005**, *32*, 9.
(52) Puleo, A. C.; Muruganandam, N.; Paul, D. R. Gas sorption and transport in substituted polystyrenes. *J. Polym. Sci., Part B: Polym. Phys.* **1989**, *27*, 2385−2406.
(53) Zoller, P.; Walsh, D. J. *Standard pressure-volume-temperature data for polymers*; Technomic Publishing Company, Inc.: Lancaster, PA, 1995.
(54) Zhou, N. C.; Chan, C. D.; Winey, K. I. Reconciling STEM and X-ray scattering data to determine the nanoscale ionic aggregate morphology in sulfonated polystyrene ionomers. *Macromolecules* **2008**, *41*, 6134−6140.
(55) Kusuma, V. A.; Freeman, B. D.; Smith, S. L.; Heilman, A. L.; Kalika, D. S. Influence of TRIS-based co-monomer on structure and gas transport properties of cross-linked poly(ethylene oxide). *J. Membr. Sci.* **2010**, *359*, 25−36.
(56) Merten, U. *Desalination by reverse osmosis*; MIT Press: Cambridge, 1966.
(57) Wijmans, J. G.; Baker, R. W. The solution-diffusion model: A review. *J. Membr. Sci.* **1995**, *107*, 1−21.
(58) Paul, D. R. Reformulation of the solution-diffusion theory of reverse osmosis. *J. Membr. Sci.* **2004**, *241* (2), 371−386.
(59) ASTM *Standard test methods for vulcanized rubber and thermoplastic elastomers - tension*; ASTM D 412; 2006.
(60) Lonsdale, H. K.; Merten, U.; Riley, R. L. Transport properties of cellulose acetate osmotic membranes. *J. Appl. Polym. Sci.* **1965**, *9*, 1341−1362.
(61) Atkins, P.; de Paula, J. *Physical chemistry*, 7th ed.; W. H. Freeman and Company: New York, 2002.
(62) ASTM *Standard test methods for water vapor transmission of materials*; ASTM E 96; 2011.
(63) Yasuda, H.; Lamaze, C. E.; Ikenberry, L. D. Permeability of solutes through hydrated polymer membranes Part I. Diffusion of sodium chloride. *Die Makromolekulare Chemie* **1968**, *118*, 19−35.
(64) Cussler, E. L. *Diffusion: Mass transfer in fluid systems*, 2nd ed.; Cambridge University Press: New York, 2003.
(65) Pethrick, R. A. Positron annihilation - A probe for nanoscale voids and free volume? *Prog. Polym. Sci.* **1997**, *22*, 1−47.
(66) Mogensen, O. E. Spur reaction model of positronium formation. *J. Chem. Phys.* **1974**, *60* (3), 998−1004.
(67) Kansy, J. Microcomputer program for analysis of positron annihilation lifetime spectra. *Nucl. Instrum. Methods Phys. Res., Sect. A* **1996**, *374* (2), 235−244.
(68) Hill, A. J.; Freeman, B. D.; Jaffe, M.; Merkel, T. C.; Pinnau, I. Tailoring nanospace. *J. Mol. Struct.* **2005**, *739*, 173−178.
(69) Dong, A. W.; Pascual-Izarra, C.; Pas, S. J.; Hill, A. J.; Boyd, B. J.; Drummond, C. J. Positron annihilation lifetime spectroscopy (PALS) as a characterization technique for nanostructured self-assembled amphiphile systems. *J. Phys. Chem. B* **2008**, *113* (1), 84−91.
(70) Rowe, B. W.; Pas, S. J.; Hill, A. J.; Suzuki, R.; Freeman, B. D.; Paul, D. R. A variable energy positron annihilation lifetime spectroscopy study of physical aging in thin glassy polymer films. *Polymer* **2009**, *50*, 6149−6156.
(71) Ju, H.; Sagle, A. C.; Freeman, B. D.; Mardel, J. I.; Hill, A. J. Characterization of sodium chloride and water transport in poly(ethylene oxide) hydrogels. *J. Membr. Sci.* **2010**, *358*, 131−141.
(72) Park, H. B.; Jung, C. H.; Lee, Y. M.; Hill, A. J.; Pas, S. J.; Mudie, S. T.; Van Wagner, E.; Freeman, B. D.; Cookson, D. J. Polymers with cavities tuned for fast selective transport of small molecules and ions. *Science* **2007**, *318*, 254−258.
(73) Shimazu, A.; Ikeda, K.; Miyazaki, T.; Ito, K. Application of positron annihilation technique to reverse osmosis membrane materials. *Radiat. Phys. Chem.* **2000**, *58*, 555−561.
(74) Jean, Y. C. Positron annihilation spectroscopy for chemical analysis: A novel probe for microstructural analysis of polymers. *Microchem. J.* **1990**, *42* (1), 72−102.
(75) Mohamed, H. F. M.; Ito, K.; Kobayashi, Y.; Takimoto, N.; Takeoka, Y.; Ohira, A. Free volume and permeabilities of O_2 and H_2 in Nafion membranes for polymer electrolyte fuel cells. *Polymer* **2008**, *49* (13−14), 3091−3097.
(76) Mohamed, H. F. M.; Kobayashi, Y.; Kuroda, C. S.; Ohira, A. Effects of ion exchange on the free volume and oxygen permeation in Nafion for fuel cells. *J. Phys. Chem. B* **2009**, *113* (8), 2247−2252.
(77) Mohamed, H. F. M.; Ohira, A.; Kobayashi, Y. Free volume and oxygen permeability in polymers related to polymer electrolyte fuel cells. *Mater. Sci. Forum* **2009**, *607*, 58−60.
(78) Kobayashi, Y.; Mohamed, H. F. M.; Ohira, A. Positronium formation in aromatic polymer electrolytes for fuel cells. *J. Phys. Chem. B Lett.* **2009**, *113*, 5698−5701.
(79) Tung, K.-L.; Jean, Y.-C.; Nanda, D.; Lee, K.-R.; Hung, W.-S.; Lo, C.-H.; Lai, J.-Y. Characterization of multilayer nanofiltration

membranes using positron annihilation spectroscopy. *J. Membr. Sci.* **2009**, *343*, 147−156.
(80) Pascual-Izarra, C.; Dong, A. W.; Pas, S. J.; Hill, A. J.; Boyd, B. J.; Drummond, C. J. Advanced fitting algorithms for analysing positron annihilation lifetime spectra. *Nucl. Instrum. Methods Phys. Res., Sect. A* **2009**, *603* (3), 456−466.
(81) Tao, S. J. Positronium annihilation in molecular substances. *J. Chem. Phys.* **1972**, *56*, 5499−5510.
(82) Eldrup, M.; Lightbody, D.; Sherwood, J. N. The temperature dependence of positron lifetimes in solid pivalic acid. *Chem. Phys.* **1981**, *63* (1−2), 51−58.
(83) Mallon, P. E., Application to polymers. In *Principles and applications of positron & positronium chemistry*; Jean, Y. C., Mallon, P. E., Schrader, D. M., Eds.; World Scientific Publishing Co.: Singapore, 2003; pp 253−280.
(84) MaCKenzie, K. J. D.; Smith, M. E. In *Multinuclear Solid State NMR of Inorganic Materials*; Pergamon: New York, 2002; Chapter 5.
(85) Silverstein, R. M.; Webster, F. X.; Kiemle, D. J. *Spectrometric identification of organic compounds*, 7th ed.; John Wiley & Sons Inc.: Hoboken, NJ, 2005.
(86) Pitzer, K. S.; Peiper, J. C.; Busey, R. H. Thermodynamic properties of aqueous sodium chloride solutions. *J. Phys. Chem. Ref. Data* **1984**, *13* (1), 1−102.
(87) Bonner, O. D.; Payne, W. H. Equilibrium studies of some univalent ions on Dowex 50. *J. Phys. Chem.* **1954**, *58*, 183−185.
(88) Flory, P. J. Thermodynamics of high polymer solutions. *J. Chem. Phys.* **1942**, *10*, 51−61.
(89) Thorsen, T.; Holt, T. The potential for power production from salinity gradients by pressure retarded osmosis. *J. Membr. Sci.* **2009**, *335*, 103−110.
(90) Cath, T., Y.; Childress, A. E.; Elimelech, M. Forward osmosis: Principles, applications, and recent developments. *J. Membr. Sci.* **2006**, *281*, 70−87.
(91) McCutcheon, J. R.; McGinnis, R. L.; Elimelech, M. A novel ammonia-carbon dioxide forward (direct) osmosis desalination process. *Desalination* **2005**, *174*, 1−11.
(92) Achilli, A.; Cath, T. Y.; Childress, A. E. Power generation with pressure retarded osmosis: An experimental and theoretical investigation. *J. Membr. Sci.* **2009**, *343* (1−2), 42−52.
(93) Lee, K. P.; Arnot, T. C.; Mattia, D. A review of reverse osmosis membrane materials for desalination - Development to date and future potential. *J. Membr. Sci.* **2011**, *370*, 1−22.
(94) Elimelech, M.; Phillip, W. A. The future of seawater desalination: Energy, technology, and the environment. *Science* **2011**, *333*, 712−717.
(95) Janssen, G. J. M.; Overvelde, M. L. J. Water transport in the proton-exchange-membrane fuel cell: Measurements of the effective drag coefficient. *J. Power Sources* **2001**, *101* (1), 117−125.
(96) Paul, D. R. Relation between hydraulic permeability and diffusion in homogeneous swollen membranes. *J. Polym. Sci., Polym. Phys. Ed.* **1973**, *11*, 289−296.
(97) Paul, D. R. Further comments on the relation between hydraulic permeation and diffusion. *J. Polym. Sci., Polym. Phys. Ed.* **1974**, *12* (6), 1221−1230.
(98) Paul, D. R., Diffusive transport in swollen polymer membranes. In *Permeability of Plastic Films and Coatings: To Gases, Vapors, and Liquids*; Hopfenberg, H. B., Ed.; Plenum Press: New York, 1974; pp 35−48.
(99) Sagle, A. C. PEG hydrogels as anti-fouling coatings for reverse osmosis membranes. Ph.D. Thesis, The University of Texas, Austin, TX, 2009.
(100) DOW^{TM} FILMTEC^{TM} Reverse Osmosis and Nanofiltration Elements. http://www.dowwaterandprocess.com/products/ronf.htm (accessed November 6, 2011).
(101) Yasuda, H.; Ikenberry, L. D.; Lamaze, C. E. Permeability of solutes through hydrated polymer membranes Part II. Permeability of water soluble organic solutes. *Die Makromolekulare Chemie* **1969**, *125*, 108−118.
(102) Cohen, M. H.; Turnbull, D. Molecular transport in liquids and glasses. *J. Chem. Phys.* **1959**, *31* (5), 1164−1169.
(103) Sagle, A. C.; Ju, H.; Freeman, B. D.; Sharma, M. M. PEG-based hydrogel membrane coatings. *Polymer* **2009**, *50*, 756−766.
(104) Paul, M.; Park, H. B.; Freeman, B. D.; Roy, A.; McGrath, J. E.; Riffle, J. S. Synthesis and crosslinking of partially disulfonated poly(arylene ether sulfone) random copolymers as candidates for chlorine resistant reverse osmosis membranes. *Polymer* **2008**, *49*, 2243−2252.
(105) Kim, Y.-J.; Lee, K.-S.; Jeong, M.-H.; Lee, J.-S. Highly chlorine-resistant end-group crosslinked sulfonated-fluorinated poly(arylene ether) for reverse osmosis membrane. *J. Membr. Sci.* **2011**, *378*, 512−519.
(106) Glueckauf, E. A new approach to ion-exchange polymers. *Proc. R. Soc. London, Ser. A* **1962**, *268*, 350−370.
(107) Geise, G. M. *Unpublished Data*, The University of Texas at Austin, Austin, TX, 2011.
(108) Yasuda, H.; Lamaze, C. E. *Improved membranes for reverse osmosis*; Office of Saline Water Research and Development Progress Report No. 473; U.S. Department of the Interior: Washington, DC, 1969.
(109) Fell, C. J. D.; Hutchison, H. P. Diffusion coefficients for sodium and potassium chlorides in water at elevated temperatures. *J. Chem. Eng. Data* **1971**, *16* (4), 427−429.
(110) Eldrup, M.; Mogensen, O. Positron lifetimes in pure and doped ice and in water. *J. Chem. Phys.* **1972**, *57* (1), 495−504.